Chapter 4

Calibration of the Hot-film Sensors

The hot-film sensors that are used in the actual tests have been calibrated for each roll angle position of the model at zero angle of attack in the Stability Wind Tunnel. During the calibrations, for the sail-on-side case, axis-symmetric flow around the model was maintained by removing the sail. The boundary layer velocity profiles were obtained on the constant diameter region of the model at $0°$ angle of attack in the Open-throat tunnel of Virginia Tech. Boundary layer properties calculated from these velocity profiles were used in the calibration procedure. The details about the calibration process are presented in this chapter.

4.1 Description of the Experimental Apparatus

Boundary Layer velocity profile measurements were performed in the Open-throat tunnel of the Virginia Tech Aerospace and Ocean Engineering Department. The Open-throat wind tunnel is a wooden, circular, return type tunnel with an open test section. Detailed description of the tunnel can be found on the AOE Web page. In recent years, flow quality of the tunnel has been improved by installing a screen to make the flow exit the nozzle more uniform and by building a vent to bleed the same amount of air that is entrained at the test section [21]. The valve on the top of the vent box was kept open during all the runs in order to make use of this improvement. One disadvantage of the tunnel is the temperature control. It has been seen that it was difficult to keep the temperature constant, however temperature change was not high enough to effect the velocity profile measurements.

A support assembly, as shown in figure 4.1, was build in order to place the model in the Open-throat tunnel. This assembly consists of two wooden supports each connected to the lower tunnel walls through two steel legs. The model was placed on the wooden supports in such a way that the whole part of the constant diameter region could be remained in the test section. The centerline of the model and the support assembly in the Y-direction was aligned with the centerline of the tunnel in the Y direction. However, center of symmetry of the model was shifted up from the center of the tunnel with a certain distance in order to minimize the blockage effects and keep the flow axis-symmetric around the constant diameter part of the model. Keeping the flow axis-symmetric is an important task, since all the theoretical calculations used to determine the skin-friction distribution are based upon this assumption. To find the magnitude of the shift distance in the Y-direction, center of the cross-sectional area of the model with the wooden block and the legs in the Y-Z plane has been calculated and this center is aligned with the center of the tunnel. As a result, a shift distance of 3.22 inches in the Y-direction has been found.

After the model was placed on the supports, velocity measurements were made with a Pitot tube in eight stations to check the symmetry of the flow. These eight stations were taken on a circle of radius 30 inches and each station was 45° apart from the next station in the circumferantial direction as shown in figure 4.2. (Note that streamwise direction X is into the page in figures 4.1 and 4.2). The results are plotted in figure 4.3. As can be seen from this plot, the velocity difference in each station is in acceptable limits and flow can be regarded as axis-symmetric.

Boundary layer velocity profiles were obtained by using a boundary layer type pitot probe with a tip diameter of 0.035 inches. The boundary layer probe was moved in the normal direction to the wall by using an electrically driven traverse mechanism. One revolution of the barrel in the traverse mechanism was equivalent to a 0.025-inch vertical move. The probe was moved in the streamwise direction by hand on an aluminum bar placed over the test section and secured in two ends on the upper tunnel walls. The pitot probe was attached to a water manometer with a resolution of 0.02 inches.

4.2 Boundary Layer Velocity Profile Measurements

Boundary layer velocity profiles on the constant diameter region of the model were taken in four different speeds: 60 ft/s (18.3 m/s), 80 ft/s (24.4 m/s), 95 ft/s (28.9 m/s) and 110 ft/s (33.5 m/s). Measurements were made in two stations located on the first sensor row for each speed. As can be seen from figure 4.4, the first station is at the upstream location of the constant diameter region ($x/L = 0.25$) and the second station at the downstream part ($x/L = 0.59$). Boundary layer properties obtained from the second station were used as the initial value for the theoretical calculations.

To resolve the typical regions of the turbulent velocity profiles, (semi-logarithmic region, wake region etc.) the pitot probe was moved with logarithmic increments from the wall. The readings were assumed to be started from the half of the diameter of the probe, 0.0175 inches from the wall. Therefore the data from the viscous sublayer and some part of the logarithmic region couldn't be obtained. In fact, as will be discussed in the next section, the data obtained in the vicinity of the wall weren't used in the calculation of the boundary layer properties because of the possible errors originating from the wall-probe interference.

Streamwise velocity measurements were made in 29 stations to determine the boundary layer edge velocity U_e distribution for each speed. First and the last stations are the same as the first and the second stations used in the boundary layer traverses. From station 0 to station 27, the distance between the stations are 1 inches. The results obtained from these measurements are given in figure 4.8. As can be seen from these plots, for all the speeds, the change in U_e in the streamwise direction is negligible and can be regarded as constant.The temperature of the tunnel and the atmospheric pressure have been recorded regularly during all the runs in order to update the dynamic viscosity μ, and the density ρ of the air which were used in the theoretical calculations.

4.2.1 Boundary Layer Thickness Determination

The boundary layer thickness δ is defined as the normal distance y from the wall where $U = 0.99 \times U_e$. Here U is the streamwise velocity component and U_e is the boundary layer edge velocity. The U vs. y values have been recorded for all the profile measurements and the value of the boundary layer edge has been determined by making linear interpolation between the appropriate values. Values of δ at the first and the second stations for each speed are given in Table 4.1.

Boundary layer thickness determination, both in experimental and numerical studies, is a difficult issue, since near the edge of the turbulent boundary layer velocity change is rather small and the uncertainties associated with the measurement technique (e.g. resolution of the anemometer or reading errors) may cause significant deviations in the determination of the δ values. Therefore, the characterization of the boundary layer profiles with the integral properties like displacement thickness δ^* and momentum thickness θ would be more appropriate.

4.2.2 Calculation of the Boundary Layer Properties

In order to calculate the boundary layer properties like δ^* and θ, the complete velocity profile should be used. However, as previously discussed, the profiles obtained experimentally didn't contain the viscous sublayer and some part of the logarithmic layer. Contributions to the calculation of the integral properties from these regions is not negligible, thus a proper method to complete the profile data should be sought. The first step is to find the friction velocity U_τ for that particular profile.

U_τ can be obtained by using the logarithmic region in a turbulent profile. In the literature one may see many ways of finding U_τ. All these methods make use of the logarithmic region. In this study curvature effects are also considered. In White [22], the logarithmic region for a turbulent profile with curvature effect is given by the equation:

$$U^+ = \frac{1}{K} ln(r^+) + A \tag{4.1}$$

where

$$U^+ = \frac{U}{U_\tau} \qquad and \qquad r^+ = \frac{aU_\tau}{\nu} ln\left(1 + \frac{y}{a}\right) \tag{4.2}$$

Also for the coefficients, K=0.41 and A=5.0 have been used (Coles and Hirst [23]). At $r^+ = 100$, equation 4.1 gives $U^+ = 16.23$. In equation 4.2, a is the radius of curvature and for our case in the constant diameter region of the model this value is 5.25 inches. For finding U_τ, the point in the velocity profile where both U and y values are satisfied is sought for $U^+ = 16.23$ and $r^+ = 100$ by changing the value of U_τ. Once the point is found, the corresponding value of U_τ is taken as the actual friction velocity for that particular profile. Two equations used in this iteration process are derived from equations 4.1 and 4.2 and given as:

$$y_{r^+=100} = 5.25 \left(e^{\frac{C\nu}{U_\tau}} \right) \tag{4.3}$$

$$U = 16.23 U_\tau \tag{4.4}$$

In equation 4.3, $C = 750.0\ m^{-1}$. Once the friction velocity is obtained, the viscous sublayer can be approximated up to $r^+ = 10$ by the equation:

$$U^+ = r^+ \tag{4.5}$$

To eliminate the bad points in the vicinity of the wall, actual experiment data with r^+ value equal to or greater than 100 are used and the region between $r^+ = 10$ and $r^+ = 100$ is approximated by the equation:

$$U^+ = 7.5333 \left(r^+\right)^{1/6} \tag{4.6}$$

In Kays and Crawford [24], this equation is given with (1/7) as the exponent and with a different constant as well. However for the profiles obtained in this study, it has been seen that (1/6) exponent form fits the data better than (1/7) exponent form for all the cases. The constant in equation 4.6 was obtained by making U^+ equal to 16.23 for $r^+ = 100$, which agrees with equation 4.1 using the Coles and Hirst [23] constants.

The above procedure has been used for obtaining the complete profile for each station and speed. The results are given in figures 4.5 to 4.7. The logarithmic region gets larger as the speed increases and particularly for a given speed the logarithmic region of the profile obtained in the second station is again larger with respect to the one obtained in the first station.

After the complete profile data for each case were obtained, boundary layer properties δ^*, θ and the shape factor H have been calculated. These properties and Re_θ, the Reynolds Number based on θ for each case are presented in table 4.1.

Although all the calibration steps described to this point have been applied to $U_e = 60$ ft/s case besides 80, 95 and 110 ft/s, boundary layer properties obtained at this particular speed were not used in the remaining calibration procedure. The velocity profiles at 60 ft/s showed transitional character. Since all the theoretical calculations in the calibration procedure were based on fully turbulent axis-symmetric flow assumption over the model, the results of the 60 ft/s case were not used in the skin-friction determination. Therefore

Table 4.1: Boundary layer properties at $U_e = 80$, 95 and 110 ft/s.

$\mathbf{U_e}$, ft/s	Station #	$\mathbf{U_\tau}$, ft/s	δ, inches	δ^*/δ	θ/δ	H	$\mathbf{Re_\theta}$
80.0	1	1.11	0.26	0.17	0.12	1.44	1114
80.0	2	0.98	0.96	0.15	0.11	1.35	3840
95.0	1	1.33	0.22	0.17	0.12	1.43	1127
95.0	2	1.13	0.96	0.15	0.11	1.34	4752
110.0	1	1.44	0.25	0.16	0.11	1.44	1470
110 .0	2	1.30	0.85	0.15	0.11	1.36	4920

actual experimental data used in the calibration procedure consist of boundary layer velocity profile measurements acquired at 80, 95 and 110 ft/s. As can be seen from table 4.1, experimental calibration C_f values were obtained for $1010 \leq Re_\theta \leq 4900$. The extension of the calibration range to 140 ft/s was achieved by using a theoretical approach described in section 3.3.

For 80, 95 and 110 ft/s, to determine the θ distribution between two measurement stations, the following momentum integral equation has been used:

$$0.03138 \left[Re_a \ln \left(1 + 9.337 \frac{\theta}{a} \right) \right]^{-0.2857} = \frac{d\theta}{dx} \tag{4.7}$$

This equation has been obtained by using the approach in Kays and Crawford [24] and making necessary modifications to include the transverse curvature effects. Equation 4.7 which represents an initial value problem, has been solved numerically by using *Modified Euler's Method* in order to determine the momentum thickness distribution. As the initial value for the momentum thickness, the θ value measured at the second station has been used.

4.3 Calculation of the Skin-Friction Values

After obtaining the θ distribution at 80, 95 and, 110 ft/s, the skin friction coefficient at each sensor location has been calculated by using the *Ludwieg-Tillmann equation* [25]:

$$\frac{C_f}{2} = 0.123 \times 10^{-0.678H} \left(\frac{U_e \theta}{\nu} \right)^{-0.268} \tag{4.8}$$

Steady and unsteady experiments over the DARPA2 model have been performed at a nominal wind tunnel speed of 140 ft/s. The wall shear stress at this speed, especially on the windward side of the model at an angle of attack, would be significantly high compared to the values obtained at the experimental calibration speeds. Since the highest calibration speed that can be reached at the open throat tunnel was 110 ft/s, the calculation of the actual shear stress in the experiments would require to approximate the values well above the skin-friction magnitudes obtained from the experimental velocity profile measurements. In order to reduce the error in the extrapolation, the skin-friction distribution at the constant diameter region of the model at 140 ft/s was approximated by using the equation given in White [26]:

$$C_f = 0.0015 + \left[0.20 + 0.016\left(\frac{x}{a}\right)^{0.4}\right] Re_x^{-1/3} \tag{4.9}$$

In the same work, White [26] showed that equation 4.9 had an rms error of ±9% compared with the available data, which was the lowest of any theory known to the author at that time.

4.4 Calculation of the Calibration Coefficients

In order to relate the voltage values acquired from the constant temperature anemometers with the wall shear values, the surface hot-film version of King's Law has been used (Bruun [27]):

$$\frac{E^2}{(T_w - T_\infty)} = A + B(\tau_w)^{1/3} \tag{4.10}$$

Here, E is the time-averaged voltage value obtained from a surface hot-film sensor connected to a constant temperature anemometer, T_w stands for the sensor temperature and T_∞ for free-stream temperature of the flow in the tunnel. The purpose of the calibration is to determine the coefficients A and B in equation 4.10. For finding these coefficients, E and the corresponding τ_w value obtained at 80, 95, 110 and 140 ft/s have been used to make a linear regression.

In equation 4.10, the change in the free-stream temperature will also cause a change in the calibration coefficients A and B. Since the temperature of the stability tunnel is ambient and cannot be controlled, the calibration procedure was repeated as the tunnel temperature changed. In order to minimize the uncertainty in the skin friction measurements due to the free-stream temperature change for the barebody case, the calibration coefficients for each sensor have been re-calculated for every roll angle position of the model before taking steady data and performing unsteady maneuvers for that specific roll angle. At each roll position of the model, the voltage values E from each sensor were acquired at 0° angle of attack for the speeds 80, 95, 110 and 140 ft/s. Since the τ_w value corresponding to each speed at all the sensor locations were known, the calibration coefficients A and B for each sensor and roll angle position could be obtained by using equation 4.10. The free-stream temperature change was at most ± 0.5 C$^\circ$ between the start of the steady measurements and the end of the unsteady maneuvers for each roll angle and this was included in the overall uncertainty calculations. For the measurements with the sail, calibration coefficients for each sensor were re-calculated approximately in every 10 roll angle by simply detaching the sail from the body and applying the calibration procedure to the barebody. Between each calibration runs, the same values of A and B coefficients were used for each sensor.

Figure 4.9 shows the skin-friction vs. x/L distribution obtained as the result of the calibration procedure at the actual experiments in the Stability Wind Tunnel at 0° angle of attack. The Reynolds number based on the model length Re_L is 5.5×10^6. In the same figure, the data are compared with the C_f values obtained at David Taylor Model Basin (DTMB) for $Re_L = 1.2 \times 10^7$ (Huang et al. [28]). Skin-friction measurements at DTMB were based on the principle that shear stress on a body in a flow can be measured with using small obstacles that stagnate the velocity field near the surface to produce a pressure rise that is approximately proportional to the shear stress. Huang et al. [28] placed small blocks with certain dimensions on the model surface near to the pressure tap locations. The pressure was measured at the tap with and without these obstacles and the measurement differences were used to compute the shear stress at that location. They reported an uncertainy of ± 0.0002 in their skin-friction measurements. Skin friction C_f vs. x/L distributions of Virginia Tech and DTMB follow the same trend. However, the magnitudes of the C_f obtained at Virginia Tech are bigger than that of DTMB. This is likely due to the difference between the Reynolds numbers and the uncertainty of the both measurements.

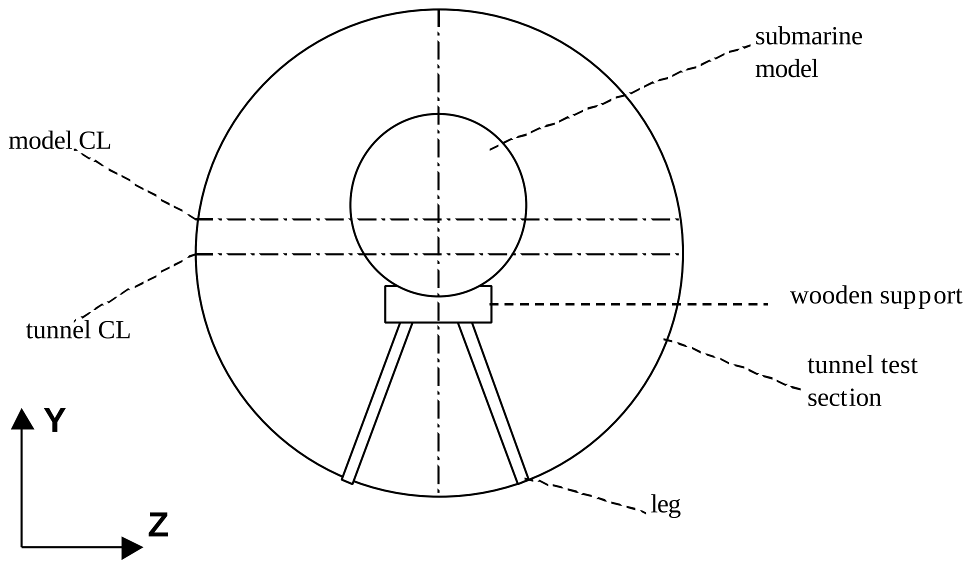

Figure 4.1: Cross-sectional view of the model and support assembly in the Y-Z plane

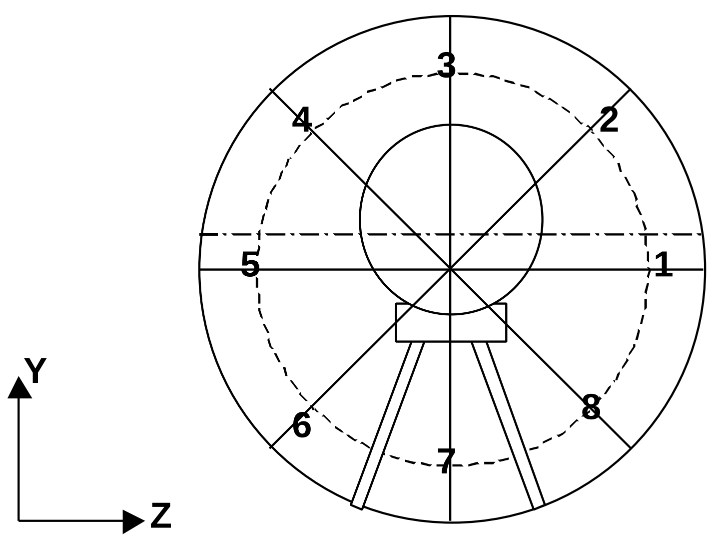

Figure 4.2: Measurement stations for the flow symmetry check

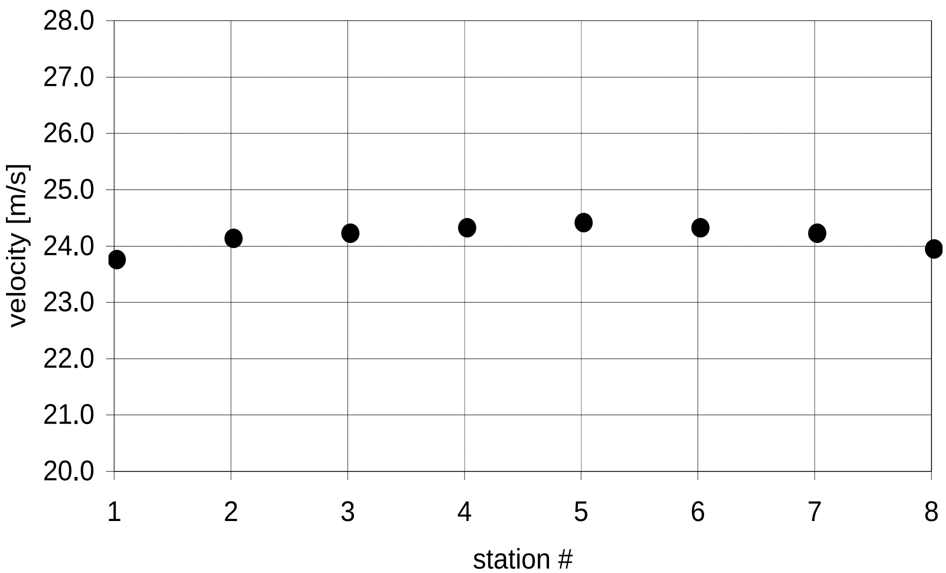

Figure 4.3: Results of the velocity measurements at the flow symmetry check points

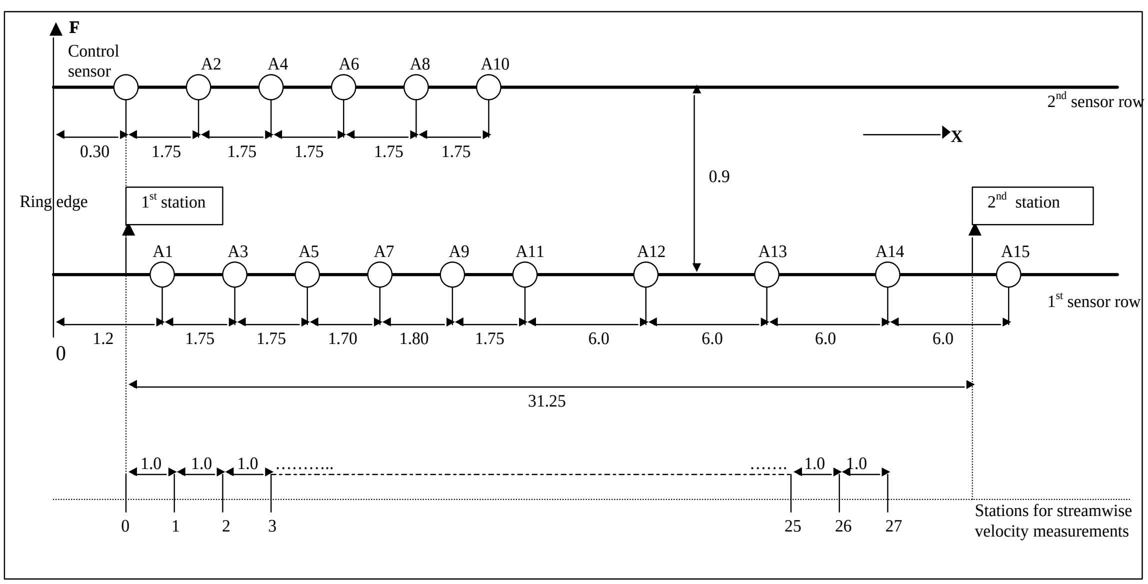

Figure 4.4: Planform view of the sensor configuration, boundary layer traverse and stremwise velocity measurement stations (all dimensions are measured in inches and the figure is not drawn to scale).

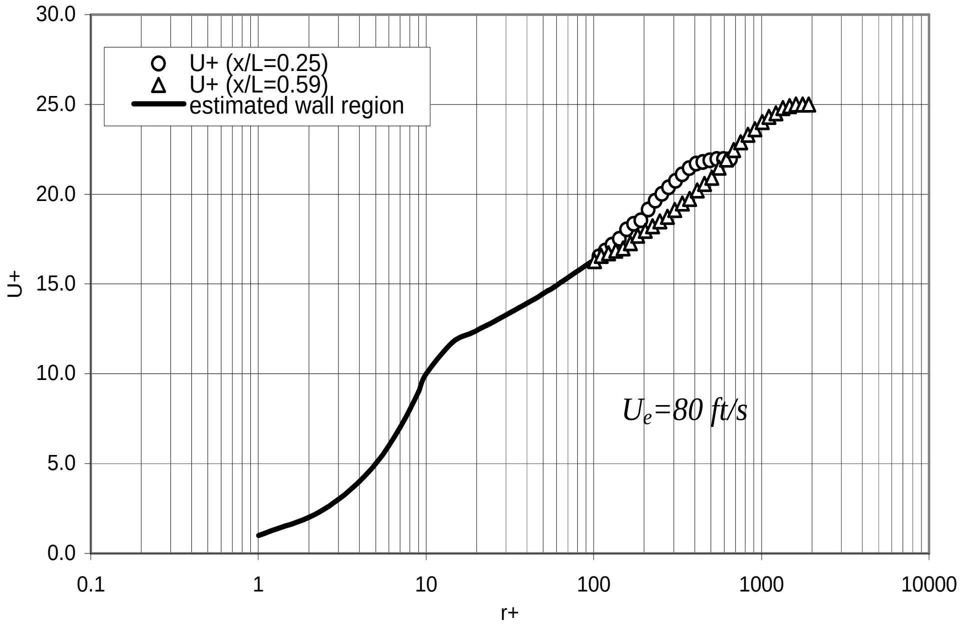

Figure 4.5: Boundary layer velocity profiles for $U_e = 80$ ft/s.

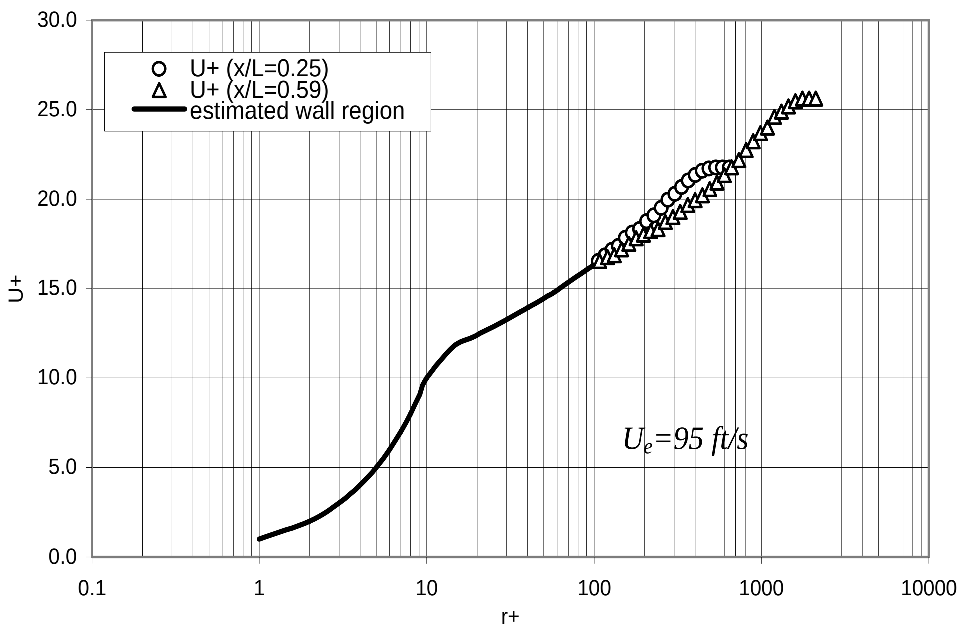

Figure 4.6: Boundary layer velocity profiles for $U_e = 95$ ft/s.

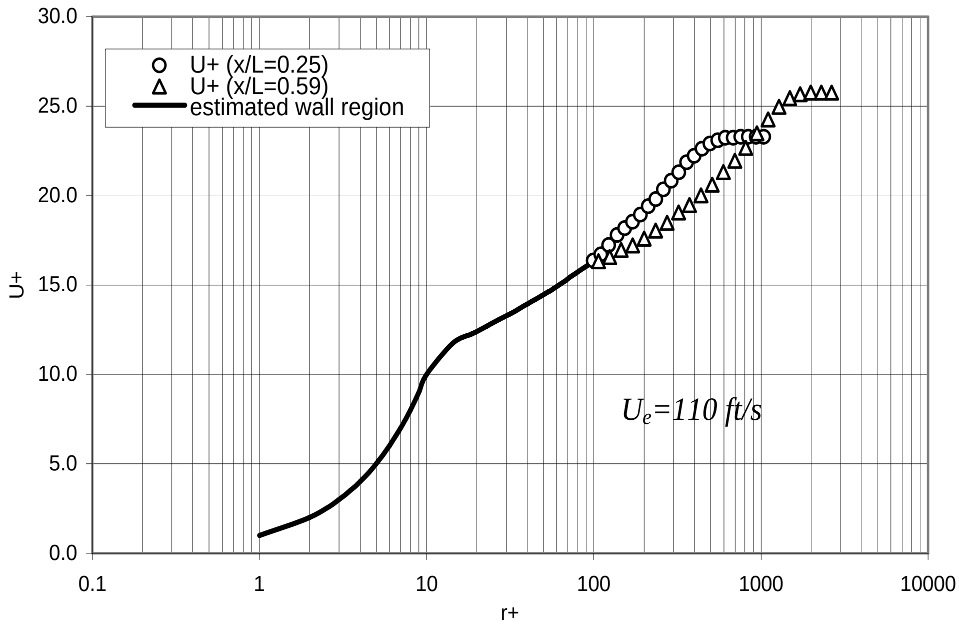

Figure 4.7: Boundary layer velocity profiles for $U_e = 110$ ft/s.

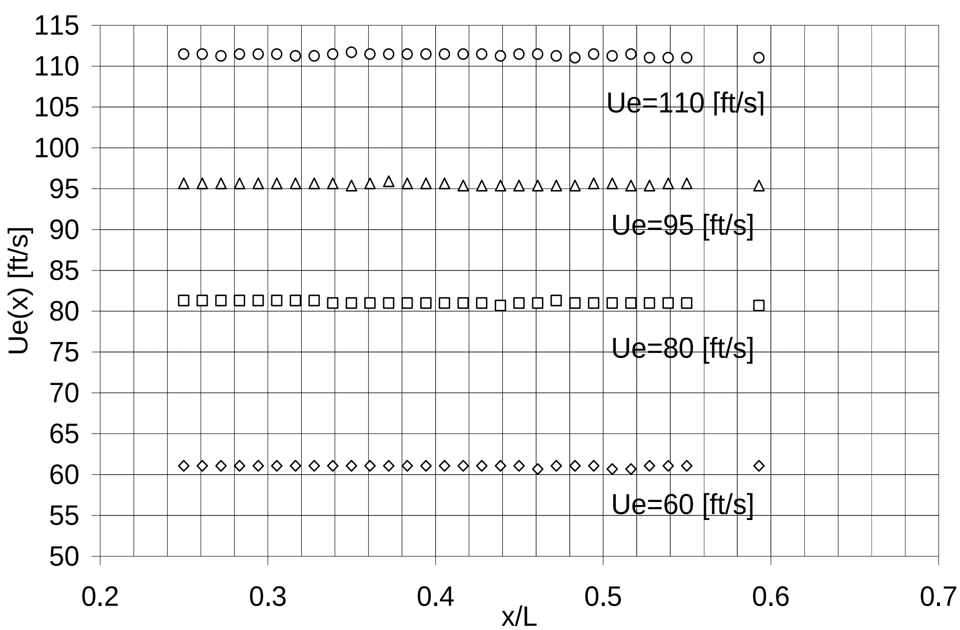

Figure 4.8: Streamwise Velocity Distributions for all calibration speeds.

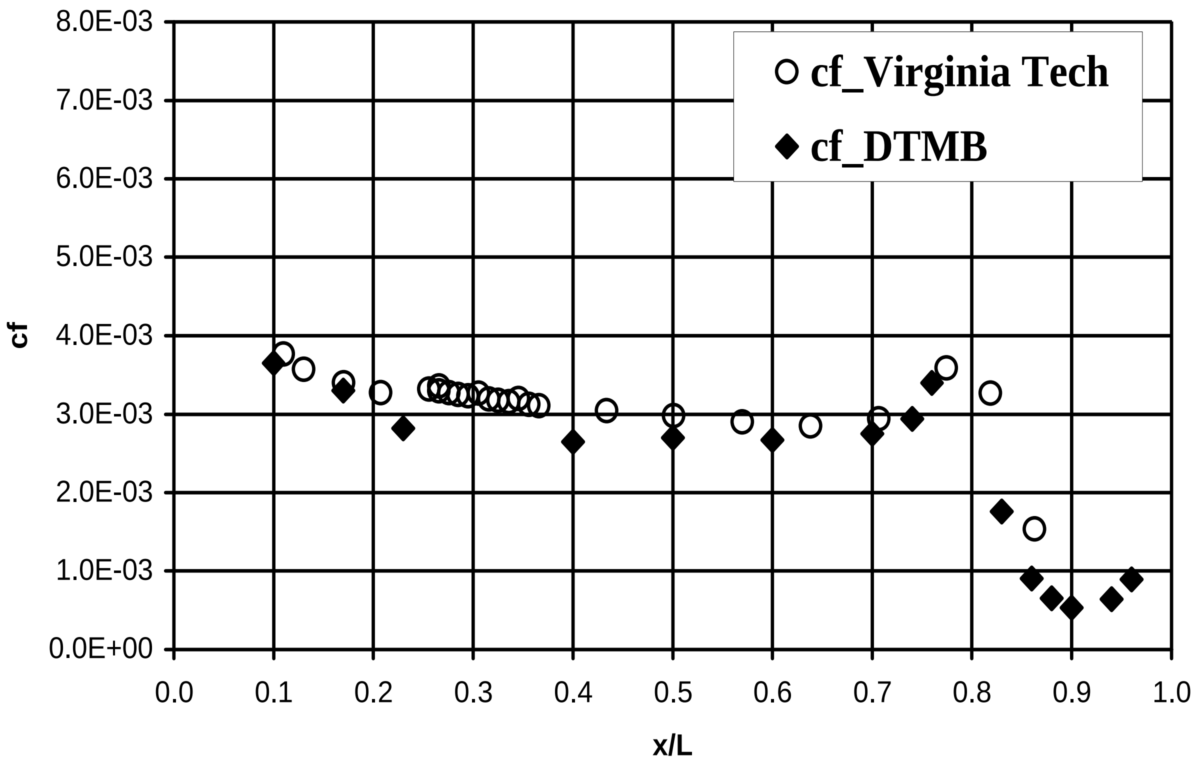

Figure 4.9: C_f vs. x/L at 0° angle of attack (For the measurements at Virginia Tech $Re_L = 5.5 \times 10^6$, for the measurements at David Taylor Model Basin (DTMB) $Re_L = 1.2 \times 10^7$)